

Journal of
***Mechanics of
Materials and Structures***

**MICROCRACK INITIATION
AT THE TIP OF A FINITE RIGID CONDUCTING LINE
IN PIEZOELECTRIC MEDIA**

Zhongmin Xiao, Hongxia Zhang and Bingjin Chen

Volume 1, N° 3

March 2006

 mathematical sciences publishers

MICROCRACK INITIATION AT THE TIP OF A FINITE RIGID CONDUCTING LINE IN PIEZOELECTRIC MEDIA

ZHONGMIN XIAO, HONGXIA ZHANG AND BINGJIN CHEN

In this paper is proposed a dislocation emission mechanism for microcrack initiation at the tip of a finite rigid conducting line in a piezoelectric solid. When a finite rigid conducting line is embedded in a piezoelectric matrix, because of the highly concentrated stress and electric displacement fields at its tips, dislocations of one sign are driven away from the tip, while the stationary dislocations of the opposite sign are left behind. As a result, a micro Zener–Stroh crack is initiated at each tip for the in-plane case, and two microcracks at each tip for the anti-plane case. We obtain analytical solutions of both in-plane and anti-plane extension forces for microcracks initiated at the tip of a finite rigid conducting line. By obtaining the stress and electric displacement fields at the tip under nonzero net Burgers vectors, we observe two critical crack lengths. We find that the in-plane and anti-plane critical extension forces for a finite rigid conducting line are related to those for a conventional crack in the same piezoelectric materials.

1. Introduction

Because of the intrinsic electromechanical coupling behavior, piezoelectric ceramics are used as actuators in adaptive structures. However, piezoelectric ceramics are very brittle and susceptible to fracture. The propagation of defects such as dislocations, cracks and inclusions would degenerate the performance of devices. It is important to understand the fracture behavior of piezoelectric ceramics.

There have been some efforts in establishing the fracture criterion for piezoelectric materials in the presence of cracks. The J integral, equal to the total potential energy release rate, has been proposed as a fracture criterion by; for example, Suo, Kuo, Barnett and Willis [Suo et al. 1992], while Pak [1990; 1992] used it to predict Mode III and Mode I fracture. However, so far there is no experimental support for this criterion. Park [1993; 1995] proposed using mechanical strain energy release

Keywords: Zener–Stroh crack, rigid line, mechanical strain energy release rate, stress and electric displacement (SED) intensity factors, piezoelectric material.

rate — the mechanical part of the total potential energy release rate — as the fracture criterion, and found that this criterion agrees qualitatively with the existing experimental observations.

Rigid line inclusions (or, for brevity, rigid lines) have been used to model certain materials or flat defects, such as metal precipitates in a piezoelectric solid. For the past decades, many researchers addressed rigid lines by solving the whole field solutions for various configurations; see, for example, [Wang et al. 1985, 1986; Li and Ting 1989; Ballarini 1990; Fan and Keer 1993; Asundi and Deng 1995]. Recently, rigid lines embedded in piezoelectric solids have been studied in [Shi 1997; Deng and Meguid 1998; Gao and Fan 2001]. All that the research work has identified is a square root singularity at the rigid line tip, and led to a stress intensity factor similar to that for a crack.

Based on those analyses, Xiao and Fan [1990] proposed a mechanism for Mode I microcrack initiation at the tip of a semi-infinite rigid line in a purely elastic solid. As a result, the fracture toughness for a rigid line was related to that for a crack in the same solid. Xiao et al. [2003] proposed a model of two Mode III microcrack initiations at the tip of a semi-infinite rigid line in a piezoelectric solid, and found the relation between the fracture toughness for a rigid line and that for a crack in the same solid. Here, the criteria of microcrack initiation at the tip of a finite rigid line in a piezoelectric solid, both for in-plane and anti-plane cases, are formally set, in analogy to crack propagation, as

$$G_+^* = G_{+cr}^* \quad \text{and} \quad G_-^* = G_{-cr}^*, \quad (1-1)$$

respectively, where G denotes the mechanical strain energy release rate when the rigid line extends, and is termed as “the rigid line extension force”; the superscript $*$ is used for a rigid line in order to distinguish it from the crack extension force; and the subscripts $+$ and $-$ represent in-plane and anti-plane cases, respectively. The two critical values G_{+cr}^* and G_{-cr}^* at the right-hand sides of Equations (1-1) are deemed to be material constants that can be determined from tests. Based on the authors’ knowledge, however, there are no such experimental results in the open literature so far. It is our conjecture that the two critical values for a rigid line can be correspondingly related to those for a crack in the same solid, since both cases associate with the square root singularity in terms of the stress and electric displacement (SED) intensity factors.

We denote by G_{+cr} and G_{-cr} the mechanical strain energy release rates of a Mode I and Mode III crack in the same piezoelectric material, respectively. Our research objective is to search for possible relations between G_{+cr}^* and G_{+cr} , as well as between G_{-cr}^* and G_{-cr} ; for example

$$G_{+cr}^* = C_1 G_{+cr} \quad \text{and} \quad G_{-cr}^* = C_2 G_{-cr}, \quad (1-2)$$

in which C_1 and C_2 are constants to be determined. To perform our investigation, models of microcrack initiation at a rigid line tip proposed by Xiao [1990; 2003] are extended to the current problems.

For the anti-plane case, a finite rigid conducting line is loaded around its two tips with the SED intensity fields $\mathbf{K}_-^* = \{K_{III}^* \ K_{D2}^*\}^T$, where K_{III}^* and K_{D2}^* are the anti-plane shear stress and electric displacement intensity factors; see Figure 1.

For the in-plane case, a finite rigid conducting line of length $2a$, perpendicular to the poling axis, is loaded at the tips by the SED intensity fields $\mathbf{K}_+^* = \{K_{II}^* \ K_I^* \ K_{D1}^*\}^T$, where K_{II}^* , K_I^* and K_{D1}^* are the in-plane shear stress, tensile stress and electric displacement intensity factors; see Figure 2.

Based on the dislocation emission mechanism at the rigid line tip proposed in [Xiao and Fan 1990; Xiao et al. 2003], dislocations of one sign are driven away from the tip of the rigid conducting line because of the concentrated fields along certain slip planes, while the dislocations with the opposite sign pile up at the tip of the rigid conducting line. As a result, Zener–Stroh cracks are initiated at both tips, as shown in Figure 3 for the anti-plane and in Figure 4 for the in-plane case.

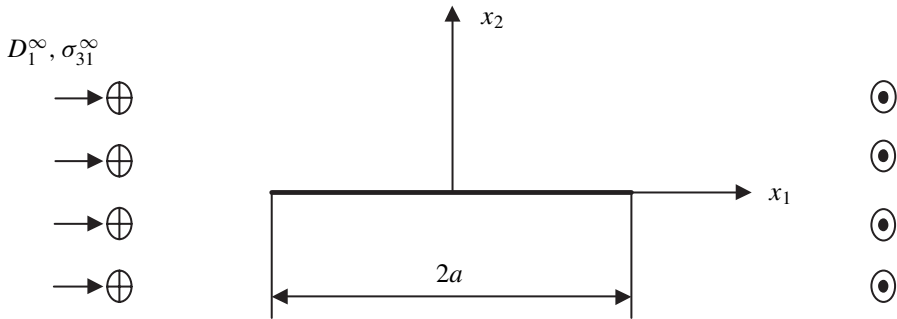


Figure 1. A finite conducting rigid line loaded around its tip with the anti-plane concentrated fields.

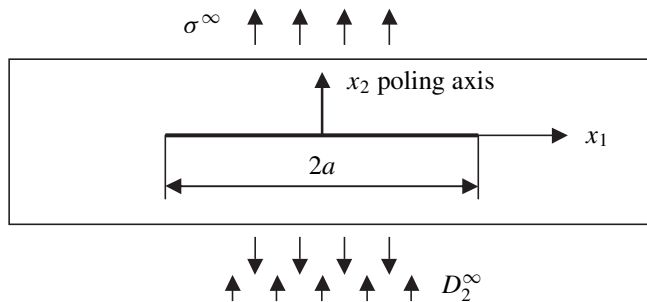


Figure 2. A finite conducting rigid line loaded around its tip with the in-plane concentrated fields.

This microcrack initiation mechanism is considered as a possible way to release the high strain energy. It is worth mentioning that this mechanism was first observed in [Kikuchi et al. 1981] and that the resulting crack was named an “anti-Zener–Stroh crack” in [Weertman 1986].

2. Formulation

2.1. Anti-plane case. In this case, because of the concentrated SED fields [Shi 1997], a pair of microcracks is initiated (see Figure 3) at both tips of the finite rigid conducting line loaded with the anti-plane SED fields \mathbf{K}_-^* (see Figure 1). We assume that the microcracks are still loaded with the tip SED fields \mathbf{K}_-^* . The pair of microcracks at one tip has the same field variables as those at the other tip, and the deformations of the two microcracks at each tip are anti-symmetric in the x_3 direction.

Here, we will analyze only the upper-right crack. The SED distributions near the right tip are approximated by $\mathbf{K}_-^*/\sqrt{2\pi y}$, with $y > 0$. We will study how a microcrack of length $2c$ is affected by the tip SED fields \mathbf{K}_-^* and by the net Burgers vectors of dislocations \mathbf{d}_T inside the microcrack.

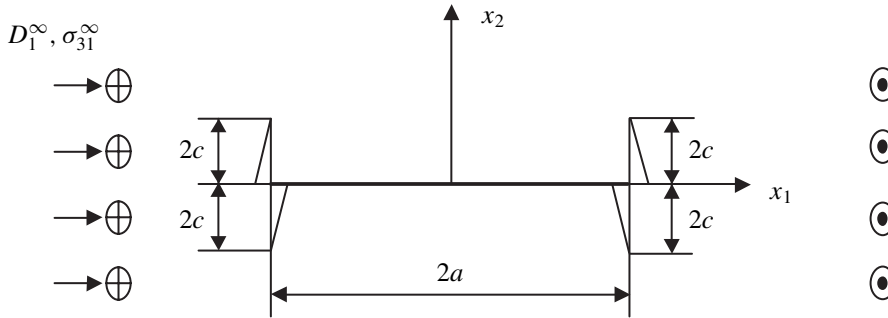


Figure 3. Microcracks initiated at the tip for the anti-plane case.

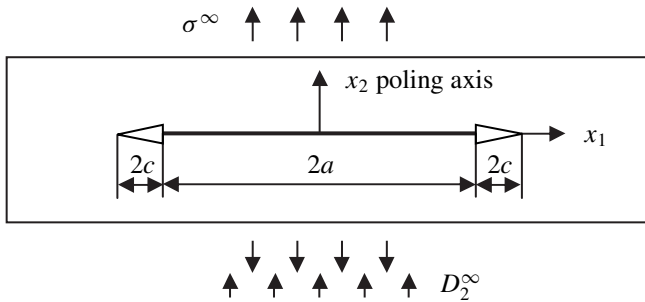


Figure 4. Microcrack initiated at the tip for the in-plane case.

The interaction between the rigid conducting line and the dislocations at both the upper and lower half-planes causes the SED fields at the upper half-plane. We first consider the two dislocations with Burgers vector $\tilde{\mathbf{d}}$, one located at the point (a, ζ) and another at $(a, -\zeta)$, $\zeta > 0$. The SED fields induced at the point (a, y) , $y > 0$, by the two dislocations interacting with the rigid conducting line [Chen et al. 2005b] take the form

$$\{\sigma_{13}(y, \zeta) \ D_1(y, \zeta)\}^T|_{x=a} = \frac{1}{4\pi} \mathbf{C} \left(-\frac{1}{y-\zeta} - \frac{1}{y-\zeta} \sqrt{\frac{\zeta}{y}} h_1(y, \zeta, a) + h_5(y, \zeta, a) \right) \tilde{\mathbf{d}}(\zeta),$$

where $h_1(y, \zeta, a)$ and $h_5(y, \zeta, a)$ are given in Appendix B, and where the material property matrix \mathbf{C} is

$$\mathbf{C} = \begin{bmatrix} c_{44} & e_{15} \\ e_{15} & -\varepsilon_{11} \end{bmatrix},$$

with c_{44} , e_{15} and ε_{11} being the elastic, piezoelectric and dielectric constants.

Because of a continuous distribution of dislocations, the SED fields along the upper-right crack line are given by

$$\{\sigma_{13}(a, y) \ D_1(a, y)\}^T = \frac{1}{4\pi} \mathbf{C} \int_0^{2c} \left(-\frac{1}{y-\zeta} - \frac{1}{y-\zeta} \sqrt{\frac{\zeta}{y}} h_1(y, \zeta, a) + h_5(y, \zeta, a) \right) \tilde{\mathbf{D}}(\zeta) d\zeta,$$

where the density vector of the charged screw dislocations along the crack line is $\tilde{\mathbf{D}}(\zeta) = \{\tilde{D}_3(\zeta) \ \tilde{D}_4(\zeta)\}^T$, with $\tilde{D}_4(\zeta) = \tilde{D}_\varphi(\zeta)$.

With the assumption that the microcrack faces are free from surface traction and charge, we have

$$\{\sigma_{13}(a, y) \ D_1(a, y)\}^T = -\frac{\mathbf{K}_-^*}{\sqrt{2\pi y}}, \quad 0 \leq y \leq 2c. \tag{2-1}$$

Moreover, the charged screw dislocation densities along the crack line must satisfy

$$\int_0^{2c} \tilde{D}_i(\zeta) d\zeta = d_{x_i}^T, \quad i = 3, 4, \tag{2-2}$$

with the net Burgers vector inside the microcrack $\mathbf{d}_T = \{d_{x_3}^T \ d_{x_4}^T\}^T$ and $d_{x_4}^T = d_\varphi^T$.

Introduce the substitutions

$$u = \frac{y}{c} - 1, \quad r = \frac{\zeta}{c} - 1.$$

Equations (2-1) and (2-2) are then rewritten as

$$\begin{aligned} \frac{1}{4\pi} \sum_{j=3}^4 C_{(i-2)(j-2)} \int_{-1}^1 \tilde{D}_j(r) \left(-\frac{1}{u-r} - \frac{1}{u-r} \tilde{h}_1\left(u, r, \frac{c}{a}\right) + \tilde{h}_5\left(u, r, \frac{c}{a}\right) \right) dr \\ = -\frac{\hat{K}_i^*}{\sqrt{2\pi c}} \frac{1}{\sqrt{u+1}}, \quad -1 \leq u, r \leq 1, \quad i = 3, 4, \quad (2-3) \end{aligned}$$

and

$$\int_{-1}^1 \tilde{D}_i(r) dr = \frac{d_{x_i}^T}{c}; \quad i = 3, 4, \quad (2-4)$$

where $\tilde{h}_1(u, r, c/a)$ and $\tilde{h}_5(u, r, c/a)$ are given in Appendix B, and

$$\hat{K}_3^* = K_{III}^*, \quad \hat{K}_4^* = K_{D2}^*.$$

2.2. In-plane case. The physical problem that we examine is shown in Figure 2: a finite rigid conducting line of length $2a$, loaded with the in-plane SED fields \mathbf{K}_+^* in a piezoelectric solid. As discussed in Section 1, because of the concentrated SED fields that we mentioned and were obtained by Deng and Meguid [1998], dislocations of one sign move away from the rigid line tips, and the left-behind dislocations form a microcrack at each tip, as shown in Figure 4. We assume that the microcracks are still controlled by the tip fields \mathbf{K}_+^* . Since the physical properties of the two microcracks are the same, we only study the one on the right. The SED distributions near the right tip are approximated by $\mathbf{K}_+^*/\sqrt{2\pi(x-a)}$, with $x > a$. We study how a microcrack of length $2c$ is affected by the tip fields \mathbf{K}_+^* and the net Burgers vectors of the dislocations \mathbf{b}_T inside the microcrack.

Based on [Chen et al. 2005a], the SED fields, arising along the crack line because of the interaction between a single charged edge dislocation located at the point $(2a + \xi, 0)$ with the Burgers vector $\tilde{\mathbf{b}}$ and with the finite rigid conducting line, are given by

$$\mathbf{\Pi}_2(x, \xi)|_{y=0} = \frac{1}{4\pi} \frac{\tilde{\mathbf{b}}(\xi)}{x - \xi} \left(\hat{\mathbf{W}} - \tilde{\mathbf{W}} \sqrt{\frac{\xi^2 - a^2}{x^2 - a^2}} \right) - \frac{1}{4\pi} \frac{\tilde{\mathbf{W}}\tilde{\mathbf{b}}(\xi)}{\sqrt{x^2 - a^2}},$$

where $\mathbf{\Pi}_2 = \{\sigma_{21} \quad \sigma_{22} \quad D_2\}^T$. The real 3×3 matrices $\hat{\mathbf{W}}$ and $\tilde{\mathbf{W}}$ are given by

$$\hat{\mathbf{W}} = \tilde{\mathbf{H}}^{-1} - \tilde{\mathbf{H}}^{-1}\tilde{\mathbf{S}}^2 + \tilde{\mathbf{L}}, \quad \tilde{\mathbf{W}} = \tilde{\mathbf{H}}^{-1} - \tilde{\mathbf{H}}^{-1}\tilde{\mathbf{S}}^2 - \tilde{\mathbf{L}},$$

while the real 3×3 matrices $\tilde{\mathbf{H}}, \tilde{\mathbf{S}}, \tilde{\mathbf{L}}$ can be obtained by removing the third column and the third row of the real 4×4 matrices $\mathbf{H}, \mathbf{S}, \mathbf{L}$ (see Appendix A). Because of a continuous distribution of dislocations along the crack line, the SED fields are

given by

$$\mathbf{\Pi}_2(x, 0) = \frac{1}{4\pi} \left(\int_a^{a+2c} \frac{\tilde{\mathbf{B}}(\xi)}{x-\xi} \left(\widehat{\mathbf{W}} - \check{\mathbf{W}} \sqrt{\frac{\xi^2 - a^2}{x^2 - a^2}} \right) d\xi - \int_a^{a+2c} \frac{\check{\mathbf{W}} \tilde{\mathbf{B}}(\xi)}{\sqrt{x^2 - a^2}} d\xi \right), \quad (2-5)$$

where the density vector of the charged edge dislocations along the microcrack line is $\tilde{\mathbf{B}}(\xi) = \{B_{x_1}(\xi) \ B_{x_2}(\xi) \ B_\varphi(\xi)\}^T$, with $B_{x_3}(\xi) = B_\varphi(\xi)$.

The boundary conditions on the crack faces in piezoelectric solids are assumed to be free of surface traction and charge [Deeg 1980; Pak 1990]. Therefore, one has

$$\mathbf{\Pi}_2(x, 0) = - \frac{\mathbf{K}_+^*}{\sqrt{2\pi(x-a)}}, \quad a \leq x \leq a + 2c. \quad (2-6)$$

The charged edge dislocation densities must satisfy

$$\int_a^{a+2c} \tilde{\mathbf{B}}(\xi) d\xi = \mathbf{b}_T, \quad (2-7)$$

where the net Burgers vector inside the crack are $\mathbf{b}_T = \{b_{x_1}^T \ b_{x_2}^T \ b_\varphi^T\}^T$, with $b_{x_3}^T = b_\varphi^T$.

The integral over $[a, a + 2c]$ is normalized to $[-1, 1]$ by the substitutions

$$t = \frac{x-a}{c} - 1, \quad s = \frac{\xi-a}{c} - 1.$$

Equations (2-6) and (2-7) now read

$$\begin{aligned} & \sum_{i=1}^3 \left(\widehat{W}_{mi} \int_{-1}^1 \frac{\tilde{B}_{x_i}(s)}{t-s} ds \right. \\ & \quad \left. - \check{W}_{mi} \int_{-1}^1 \frac{G_1(t, c/a) \tilde{B}_{x_i}(s)}{G_3(s, c/a) (t-s)} ds - \check{W}_{mi} \int_{-1}^1 G_1(t, c/a) \tilde{B}_{x_i}(s) ds \right) \\ & = -\sqrt{\frac{8\pi}{c}} G_2(t) \tilde{K}_m^*, \quad -1 \leq s, t \leq 1, \quad m = 1, 2, 3 \end{aligned} \quad (2-8)$$

and

$$\int_{-1}^1 \tilde{B}_{x_i}(s) ds = \frac{b_{x_i}^T}{c}, \quad i = 1, 2, 3, \quad (2-9)$$

where

$$\tilde{K}_1^* = K_{II}^*, \quad \tilde{K}_2^* = K_I^*, \quad \tilde{K}_3^* = K_{D1}^*,$$

$$G_1(t, c/a) = \frac{1}{\sqrt{1+t}\sqrt{1+t+2a/c}},$$

$$G_2(t) = \frac{1}{\sqrt{1+t}}, \quad G_3(s, c/a) = \frac{1}{\sqrt{1+s}\sqrt{1+s+2a/c}}.$$

3. Numerical Procedure

Let $\Psi(s)$ and $\Xi(r)$ be bounded functions in $[-1, 1]$, and the charged edge and screw dislocation density vectors can be written as

$$\begin{aligned} \tilde{\mathbf{B}}(s) &= \Psi(s) (1+s)^\alpha (1-s)^\beta, \\ \tilde{\mathbf{D}}(r) &= \Xi(r) (1+r)^\lambda (1-r)^\gamma, \end{aligned}$$

with

$$\begin{aligned} \Psi(s) &= \{\Psi_1(s) \ \Psi_2(s) \ \Psi_\varphi(s)\}^T, \quad \Psi_3(s) = \Psi_\varphi(s), \\ \Xi(r) &= \{\Xi_3(r) \ \Xi_4(r)\}^T, \quad \Xi_4(r) = \Xi_\varphi(r). \end{aligned}$$

3.1. Anti-plane case. The discretized forms of Equations (2-3) and (2-4) are written

$$\begin{aligned} \frac{1}{4\pi} \sum_{j=1}^n \tilde{W}_j(r_j) \sum_{k=3}^4 C_{(r-2)(k-2)} \Xi_k(r_j) \left(-\frac{1+\tilde{h}_1(u_i, r_j, c/a)}{u_i-r_j} + \tilde{h}_5(u_i, r_j, c/a) \right) \\ = -\frac{\hat{K}_r^*}{\sqrt{2\pi c}} \frac{1}{\sqrt{1+u_i}}, \quad -1 \leq u, r \leq 1, \quad r = 3, 4, \quad (3-1) \end{aligned}$$

and

$$\sum_{j=1}^n \tilde{W}_j(r_j) \Xi_r(r_j) = \frac{d_{x_r}^T}{c}, \quad r = 3, 4, \quad (3-2)$$

where r_j and u_i are the roots of the Jacobi polynomials,

$$P_n^{(\lambda, \gamma)}(r_j) = 0, \quad P_{n+\lambda+\gamma}^{(-\gamma, -\lambda)}(u_i) = 0, \quad j = 1, \dots, n, \quad i = 1, \dots, n-1, \quad (3-3)$$

and $\tilde{W}_j(r_j)$ can be obtained from the right-hand side of Equation (3-15) by replacing s_r, α, β with r_j, λ, γ , respectively.

Equations (3-1) and (3-2) provide a system of $2n$ linear algebraic equations to solve the $2n$ unknowns $\Xi_i(r_j)$, $i = 3, 4$, $j = 1, 2, \dots, n$. If $\Xi_i^{(1)}(r)$ and $\Xi_i^{(2)}(r)$ are the solutions of the system

$$\begin{cases} \sum_{j=1}^n \tilde{W}_j(r_j) \Xi_m^{(\gamma)}(r_j) \left(-\frac{1+\tilde{h}_1(u_i, r_j, c/a)}{u_i-r_j} + \tilde{h}_5(u_i, r_j, c/a) \right) = \frac{1}{\sqrt{1+u_i}} \delta_{1\gamma} \\ \sum_{j=1}^n \tilde{W}_j(r_j) \Xi_m^{(\gamma)}(r_j) = \delta_{2\gamma}, \quad m = 3, 4 \end{cases}$$

we obtain

$$\Xi_3^{(1)}(r) = \Xi_4^{(1)}(r) \quad \text{and} \quad \Xi_3^{(2)}(r) = \Xi_4^{(2)}(r), \tag{3-4}$$

$$\Xi_3(r) = -\sqrt{\frac{8\pi}{c}} \frac{\epsilon_{11}K_{III}^* + e_{15}K_{D2}^*}{c_{44}\epsilon_{11} + e_{15}^2} \Xi_3^{(1)}(r) + \frac{d_{x_3}^T}{c} \Xi_3^{(2)}(r), \tag{3-5}$$

$$\Xi_4(r) = -\sqrt{\frac{8\pi}{c}} \frac{e_{15}K_{III}^* - c_{44}K_{D2}^*}{c_{44}\epsilon_{11} + e_{15}^2} \Xi_4^{(1)}(r) + \frac{d_{\varphi}^T}{c} \Xi_4^{(2)}(r). \tag{3-6}$$

Since there is a square root singularity at the upper tip of the upper-right microcrack, we take $\gamma = -1/2$. As the deformations of the rigid line tip at the upper and lower half-planes are antisymmetric along the x_3 axis, we take $\lambda = -1/2$. The effect of this approximation on the upper tip is reasonably negligible [He et al. 1991].

The anti-plane SED intensity factors $\mathbf{K}_- = \{K_{III} \ K_{D2}\}^T$ at the upper tip of the upper-right microcrack are obtained as

$$\mathbf{K}_- = \lim_{y \rightarrow 2c^+} \sqrt{2\pi(y - 2c)} \{\sigma_{13}(y) \ D_1(y)\}^T = -\sqrt{\frac{\pi c}{4}} \mathbf{C} \Xi(1), \tag{3-7}$$

where K_{III} and K_{D2} are the anti-plane shear stress and electric displacement intensity factors. Combining (3-7) with (3-4), (3-5), and (3-6) leads to

$$K_{III} = \sqrt{2\pi} \Xi_3^{(1)}(1) K_{III}^* - \frac{\sqrt{\pi}}{2\sqrt{c}} \left(c_{44} \Xi_3^{(2)}(1) d_{x_3}^T + e_{15} \Xi_4^{(2)}(1) d_{\varphi}^T \right), \tag{3-8}$$

$$K_{D2} = \sqrt{2\pi} \Xi_4^{(1)}(1) K_{D2}^* - \frac{\sqrt{\pi}}{2\sqrt{c}} \left(e_{15} \Xi_3^{(2)}(1) d_{x_3}^T - \epsilon_{11} \Xi_4^{(2)}(1) d_{\varphi}^T \right). \tag{3-9}$$

According to [Park and Sun 1995], the anti-plane crack extension force can be defined as

$$G_{M-} = \lim_{\delta \rightarrow 0} \frac{1}{\delta} \int_0^{\delta} \sigma_{13}(y) u_3(\delta - y) dy.$$

Thus, the anti-plane microcrack extension force is obtained, in terms of the SED intensity factors, as

$$G_{M-} = \frac{\epsilon_{11}(K_{III})^2 + e_{15}K_{III}K_{D2}}{2(c_{44}\epsilon_{11} + e_{15}^2)}. \tag{3-10}$$

The anti-plane extension force for the finite rigid conducting line loaded with the SED intensity fields \mathbf{K}_-^* , is obtained as

$$G_{M-}^* = -\frac{\epsilon_{11}(K_{III}^*)^2 + e_{15}K_{III}^*K_{D2}^*}{2(c_{44}\epsilon_{11} + e_{15}^2)}. \tag{3-11}$$

Combined with (3-8), (3-9), and (3-11), Equation (3-10) is rewritten as

$$\begin{aligned}
 G_{M-} = & - \left(\sqrt{2\pi} \Xi_3^{(1)}(1) \right)^2 G_{M-}^* \\
 & - \frac{\pi \sqrt{\pi}}{\sqrt{2c}} \Xi_3^{(1)}(1) \Xi_3^{(2)}(1) \left(K_{III}^* d_{x_3}^T + \frac{(c_{44} d_{x_3}^T + e_{15} d_\varphi^T) (\varepsilon_{11} K_{III}^* + e_{15} K_{D2}^*)}{2 (c_{44} \varepsilon_{11} + e_{15}^2)} \right) \\
 & + \frac{\pi \left(\Xi_3^{(2)}(1) \right)^2}{8c} \left(c_{44} (d_{x_3}^T)^2 + e_{15} d_{x_3}^T d_\varphi^T \right). \tag{3-12}
 \end{aligned}$$

Note that $\Xi_j^{(u)}(1) \approx \Xi_j^{(u)}(r_1)$ for large n . In our calculation, we took $n = 100$. It is observed from Equation (3-4) that the coefficients $\Xi_3^{(1)}(1)$, $\Xi_4^{(1)}(1)$, $\Xi_3^{(2)}(1)$ and $\Xi_4^{(2)}(1)$ depend on the ratio of the microcrack's length of $2c$ to the rigid line's length of $2a$, but are independent of the material's property constants. This makes it possible to find the constant C_2 from Equation (3-12) that exhibits the relationship among the microcrack extension force G_{M-} , the rigid line extension force G_{M-}^* , the SED intensity factors \mathbf{K}_-^* , the net Burgers vectors \mathbf{d}_T , and the microcrack length $2c$. Here are the anti-plane coefficients corresponding to the ratio $c/a = 10^{-4}$:

$$\begin{aligned}
 \Xi_3^{(1)}(1) = \Xi_4^{(1)}(1) &= 0.117764, \\
 \Xi_3^{(2)}(1) = \Xi_4^{(2)}(1) &= 0.415922.
 \end{aligned}$$

Since these coefficients depend on the ratio c/a , the constant C_2 could be a function of it.

3.2. In-plane case. Following the method in [Erdogan et al. 1973], we write the discretized forms of Equations (2-8) and (2-9) as

$$\begin{aligned}
 \frac{1}{4\pi} \sum_{r=1}^n \sum_{i=1}^3 \tilde{W}_r(s_r) \left(\frac{\widehat{W}_{mi}}{t_u - s_r} - \frac{\check{W}_{mi}}{t_u - s_r} \frac{G_1(t_u, c/a)}{G_3(s_r, c/a)} - \check{W}_{mi} G_1(t_u, c/a) \right) \Psi_i(s_r) \\
 = - \frac{\tilde{K}_m^*}{\sqrt{2\pi c}} G_2(t_u), \quad -1 \leq s, t \leq 1, \quad m = 1, 2, 3, \tag{3-13}
 \end{aligned}$$

and

$$\sum_{r=1}^n \tilde{W}_r(s_r) \Psi_i(s_r) = \frac{b_{x_i}^T}{c}, \quad i = 1, 2, 3, \tag{3-14}$$

where s_r and t_u are the roots of the Jacobi polynomials,

$$P_n^{(\alpha, \beta)}(s_r) = 0, \quad P_{n+\alpha+\beta}^{(-\beta, -\alpha)}(t_u) = 0, \quad r = 1, \dots, n, \quad u = 1, \dots, n-1,$$

	c_{11} GPa	c_{12} GPa	c_{13} GPa	c_{33} GPa	c_{44} GPa	e_{31} C/m ²	e_{33} C/m ²	e_{15} C/m ²	ε_{11} nC/V·m	ε_{33} nC/V·m
PZT-5H	126	55	53	117	35.3	-6.5	23.3	17	15.1	13.0
PZT-5	121	75.4	75.2	111	21.1	-5.4	15.8	12.3	8.11	7.35
PZT-4	139	77.8	74.3	115	25.6	-5.2	15.1	12.7	6.46	5.62
PZT-7A	148	76.8	74.2	131	25.4	-2.1	9.5	12.7	4.07	2.08

Table 1. Material properties for piezoelectric ceramics (the poling direction is along the x_3 axis).

the procedure in [Muskhelishvili 1977], one obtains

$$\mathbf{K}_+ = \frac{\sqrt{\pi c}}{4} (\widehat{\mathbf{W}} - \check{\mathbf{W}}) \Psi(1). \quad (3-21)$$

Substituting (3-17)–(3-19) into (3-21), one finds

$$K_{II} = \sqrt{2\pi} f_{11} K_{II}^* + \frac{\sqrt{\pi}}{2\sqrt{c}} f_{12} b_{x_1}^T, \quad (3-22)$$

$$K_I = \sqrt{2\pi} f_{21} K_I^* + \sqrt{2\pi} f_{22} K_{D1}^* + \frac{\sqrt{\pi}}{2\sqrt{c}} (f_{23} b_{x_2}^T + f_{24} b_{\varphi}^T), \quad (3-23)$$

$$K_{D1} = \sqrt{2\pi} f_{31} K_I^* + \sqrt{2\pi} f_{32} K_{D1}^* + \frac{\sqrt{\pi}}{2\sqrt{c}} (f_{33} b_{x_2}^T + f_{34} b_{\varphi}^T), \quad (3-24)$$

where

$$f_{1i} = \tilde{L}_{11} \Psi_1^{(i^2)}(1), \quad i = 1, 2,$$

$$f_{ki} = \tilde{L}_{k2} \Psi_2^{(i+1)}(1) + \tilde{L}_{k3} \Psi_3^{(i+1)}(1), \quad k = 2, 3, \quad i = 1, 2,$$

$$f_{ki} = \tilde{L}_{k2} \Psi_2^{(i+2)}(1) + \tilde{L}_{k3} \Psi_3^{(i+2)}(1), \quad k = 2, 3, \quad i = 3, 4.$$

The coefficients f_{1i} , f_{2i} and f_{3i} can be determined, since $\Psi_i^{(k)}(1) \approx \Psi_i^{(k)}(s_1)$ exists for large n . Also, it is observed from Equations (3-16)–(3-19) that these coefficients depend on the ratio of the microcrack length of $2c$ to the rigid line length of $2a$. We take $n = 100$ in the following calculations, and select PZT-5H, PZT-5, PZT-4 and PZT-7A ceramics for our numerical examples, with the material constants listed in Table 1, taken from [Dunn and Taya 1994; Pak 1992].

According to [Park and Sun 1993], the crack extension force can then be calculated as the mechanical strain energy released when propagating the crack an infinitesimal distance, that is,

$$G_{M+} = \lim_{\delta \rightarrow 0} \frac{1}{\delta} \int_0^{\delta} \sigma_{2i}(x) u_i(\delta - x) dx, \quad i = 1, 2,$$

where δ is the assumed crack extension. Thus, the extension force for the microcrack, in terms of the SED intensity factors, is $G_{M+} = \frac{1}{2}(\mathbf{K}_+)^T \mathbf{L}' \mathbf{K}_+$, where the real 2×3 matrix \mathbf{L}' is obtained by removing the third row of the inverse of $\tilde{\mathbf{L}}$. Substituting into this equation the values given by (3-22)–(3-24), we get

$$G_{M+} = \frac{1}{2} 2\pi^2 (\mathbf{K}_+^*)^T \mathbf{X} \mathbf{K}_+^* + \frac{\pi\sqrt{\pi}}{\sqrt{2c}} (\mathbf{K}_+^*)^T \mathbf{Y} \mathbf{b}_T + \frac{\pi}{8c} (\mathbf{b}_T)^T \mathbf{Z} \mathbf{b}_T, \quad (3-25)$$

where \mathbf{X} , \mathbf{Y} and \mathbf{Z} are the 3×3 matrices from Appendix C.

The extension force for the rigid conducting line loaded with the tip SED intensity fields \mathbf{K}_+^* is obtained as

$$G_{M+}^* = -\frac{1}{2} (\mathbf{k}^*)^T \mathbf{H}' \mathbf{k}^*,$$

where $\mathbf{k}^* = \{k_1^* \ k_2^* \ k_3^*\}^T$ is the tip strain intensity factors and $\mathbf{K}_+^* = \tilde{\mathbf{S}}^T \tilde{\mathbf{H}}^{-1} \mathbf{k}^*$.

Equation (3-25) can be rewritten in terms of G_{M+}^* as

$$G_{M+} = -\frac{2\pi^2 \mathbf{s}^T \tilde{\mathbf{X}} \mathbf{s}}{\mathbf{H}'_{11}} G_{M+}^* + \pi^2 \mathbf{X}_{11} (K_{II}^*)^2 + \frac{\pi\sqrt{\pi}}{\sqrt{2c}} (\mathbf{K}_+^*)^T \mathbf{Y} \mathbf{b}_T + \frac{\pi}{8c} (\mathbf{b}_T)^T \mathbf{Z} \mathbf{b}_T, \quad (3-26)$$

where the 2×2 matrix $\tilde{\mathbf{X}}$ is obtained by removing the first row and the first column of the matrix \mathbf{X} , and we have $\mathbf{s}^T = \{\hat{\mathbf{S}}_{21} \ \hat{\mathbf{S}}_{31}\}^T$ with $\hat{\mathbf{S}} = \tilde{\mathbf{S}}^T \tilde{\mathbf{H}}^{-1}$.

Equation (3-26) gives the relationship among the microcrack extension force G_{M+} , the rigid line extension force G_{M+}^* , the tip SED intensity factors \mathbf{K}_+^* , the net Burgers vectors of dislocations \mathbf{b}_T inside the microcrack, and the microcrack length $2c$. The elements of \mathbf{X} , \mathbf{Y} and \mathbf{Z} for the ratio $c/a = 10^{-4}$ are listed in Table 2.

4. Discussion

4.1. Critical crack length.

Anti-plane case. Equation (3-12) suggests that the upper-right microcrack tends to reach its critical value at

$$G_{-cr} = -\left(\sqrt{2\pi} \Xi_3^{(1)}(1)\right)^2 G_{M-}^* - \frac{\pi\sqrt{\pi}}{\sqrt{2c_{cr}}} \Xi_3^{(1)}(1) \Xi_3^{(2)}(1) \left(K_{III}^* d_{x_3}^T + \frac{(c_{44} d_{x_3}^T + e_{15} d_\varphi^T) (\varepsilon_{11} K_{III}^* + e_{15} K_{D2}^*)}{2(c_{44} \varepsilon_{11} + e_{15}^2)} \right) + \frac{\pi \left(\Xi_3^{(2)}(1)\right)^2}{8c_{cr}} \left(c_{44} (d_{x_3}^T)^2 + e_{15} d_{x_3}^T d_\varphi^T \right). \quad (4-1)$$

	PZT-5H	PZT-5	PZT-4	PZT-7A
\mathbf{X}_{11}	1.448×10^{-12}	1.931×10^{-12}	1.586×10^{-12}	1.514×10^{-12}
\mathbf{X}_{22}	1.256×10^{-12}	1.667×10^{-12}	1.405×10^{-12}	1.352×10^{-12}
$\mathbf{X}_{23}(\mathbf{X}_{32})$	5.511×10^{-4}	9.200×10^{-4}	9.570×10^{-4}	1.145×10^{-3}
\mathbf{X}_{33}	2.172×10^4	2.313×10^4	3.753×10^4	8.592×10^4
\mathbf{Y}_{11}	0.182	0.172	0.174	0.174
\mathbf{Y}_{22}	0.169	0.161	0.161	0.169
\mathbf{Y}_{23}	2.730×10^{-11}	2.589×10^{-11}	2.189×10^{-11}	1.278×10^{-11}
\mathbf{Y}_{32}	6.608×10^7	7.593×10^7	9.368×10^7	1.287×10^8
\mathbf{Y}_{33}	0.020	0.024	0.024	0.017
\mathbf{Z}_{11}	2.275×10^{10}	1.540×10^{10}	1.901×10^{10}	2.006×10^{10}
\mathbf{Z}_{22}	2.246×10^{10}	1.516×10^{10}	1.805×10^{10}	2.078×10^{10}
$\mathbf{Z}_{23}(\mathbf{Z}_{32})$	3.955	2.747	20757	1.698
\mathbf{Z}_{33}	3.323×10^{-10}	2.156×10^{-10}	1.940×10^{-10}	7.054×10^{-11}

Table 2. Matrices \mathbf{X} , \mathbf{Y} and \mathbf{Z} under the ratio $c/a = 10^{-4}$.

The two critical crack lengths can be obtained from (4-1). The anti-plane tip SED fields \mathbf{K}_* and the net Burgers vector \mathbf{d}_T determine the two critical crack lengths.

In the absence of the electric field K_{D2}^* , of the electric displacement loading d_φ^T , and of the piezoelectric constant e_{15} , Equation (4-1) can be reduced to that for isotropic elastic media, as

$$G_{-cr|iso} = - \left(\sqrt{2\pi} \Xi_3^{(1)}(1) \right)^2 G_{-|iso}^* - \frac{\pi \sqrt{\pi} \Xi_3^{(1)}(1) \Xi_3^{(2)}(1)}{\sqrt{2c_{cr}}} K_{III}^* d_{x_3}^T + \frac{\pi \left(\Xi_3^{(2)}(1) \right)^2}{8c_{cr}} \mu (d_{x_3}^T)^2, \quad (4-2)$$

where $G_{-|iso}^* = - (K_{III}^*)^2 / (2\mu)$.

In-plane case. Equation (3-26) suggests that the right microcrack tends to reach its critical value at

$$G_{cr} = - \frac{2\pi^2 \mathbf{s}^T \tilde{\mathbf{X}} \mathbf{s}}{\mathbf{H}'_{11}} G_{M+}^* + \pi^2 \mathbf{X}_{11} (K_{II}^*)^2 + \frac{\pi \sqrt{\pi}}{\sqrt{2c_{cr}}} (\mathbf{K}_+^*)^T \mathbf{Y} \mathbf{b}_T + \frac{\pi}{8c_{cr}} (\mathbf{b}_T)^T \mathbf{Z} \mathbf{b}_T. \quad (4-3)$$

For a general Zener–Stroh crack, loaded with external stress and nonzero net dislocations, there are two critical crack lengths: one is stable, the other unstable [Fan 1994]. This particular physical phenomenon is also seen in Equation (4-3). The smaller critical crack length is a stable one under the Zener–Stroh mechanism.

The crack propagates until it reaches its second critical crack length, which is under the Griffith crack mechanism. Obviously, the applied SED fields \mathbf{K}_+^* at the tip and the net Burgers vectors \mathbf{b}_T inside the microcrack determine the two critical crack lengths.

The shear stress intensity factor K_{II}^* does not exist at the tip of the rigid line embedded in isotropic elastic materials subjected to remote loading. By using the solutions from [Wang et al. 1985; Li and Ting 1989], combined with the matrices \mathbf{S} , \mathbf{L} and \mathbf{H} for isotropic elastic materials given in [Li and Ting 1989], we can reduce (4-3) to

$$G_{+cr|iso} = -(\sqrt{2\pi} F_1(1))^2 \frac{(1-2\nu)^2}{3-4\nu} G_{+iso}^* + \frac{\pi\sqrt{\pi}}{\sqrt{2c_{cr}}} F_1(1) \Psi_2^{(5)}(1) K_I^* b_{x_2}^T + \frac{\pi}{8c_{cr}} \frac{\mu}{1-\nu} (\Psi_2^{(5)}(1))^2 (b_{x_2}^T)^2,$$

where

$$F_1(1) = \Psi_2^{(2)}(1) \frac{\mu}{1-\nu},$$

$$G_{+iso}^* = -\frac{1-\nu}{2\mu} \frac{3-4\nu}{(1-2\nu)^2} (K_I^*)^2, \quad 1 < 3-4\nu < 3.$$

Here are the numerical values of $F_1(1)$ for different values of Poisson’s ν , showing that effect of ν on $F_1(1)$ is quite small.

ν	$F_1(1)$	$\Psi_2^{(5)}(1)$
1/4	0.140453	0.337617
1/3	0.141730	0.328747
1/2	0.143271	0.318310

4.2. Connection constants. Consider a very brittle piezoelectric material, and assume that no dislocations are emitted from the rigid line tip and electric dislocations can be negligible, so that $b_{x_2}^T = b_{x_1}^T = b_\varphi^T = 0$ for the in-plane case and $d_{x_3}^T = d_\varphi^T = 0$ for the anti-plane case.

Anti-plane case. Equations (4-1) and (4-2) can be reduced to $G_{-cr}^* = C_2 G_{-cr}$, with

$$C_2 = -\frac{1}{(\sqrt{2\pi} \Xi_3^{(1)}(1))^2}. \tag{4-4}$$

Equation (4-4) partially confirmed our initial conjecture in the second equation in (1-2), both for brittle piezoelectric and for purely elastic materials. Since the coefficient $\Xi_3^{(1)}(1)$ is a result of the ratio c/a , the coefficient C_2 is a function of the ratio c/a . The numerical values of the coefficient C_2 for different ratio c/a are listed in Table 3. It shows that the absolute value of the coefficient C_2 decreases

with the increasing c/a , or with the microcrack propagation. It is observed that the C_2 value is almost constant when the microcrack is at the very initial stage ($c/a < 10^{-3}$). The variation of C_2 value for different ratio c/a is so small that we can consider the coefficient C_2 a constant. The C_2 value also indicated that the crack initiation will be catastrophic.

c/a	C_1	C_2
10^{-8}	-5.93064	-3.653
10^{-7}	-5.93064	-3.653
10^{-6}	-5.93064	-3.653
10^{-5}	-5.93064	-3.653
10^{-4}	-5.93064	-3.65299
$5 \cdot 10^{-4}$	-5.93064	-3.65295
10^{-3}	-5.93065	-3.6529
$5 \cdot 10^{-3}$	-5.93068	-3.65247
10^{-2}	-5.93073	-3.65193
$5 \cdot 10^{-2}$	-5.93108	-3.64749
10^{-1}	-5.9315	-3.64158
$5 \cdot 10^{-1}$	-5.93443	-3.58969
1	-5.93721	-3.56074

Table 3. The connection constants C_1 for PZT-5H and C_2 .

For ductile piezoelectric solids, the net Burgers vector \mathbf{b}_T inside the mixed mode microcrack and the net Burgers vector \mathbf{d}_T inside the Mode III microcrack are nonzero. In this case, G_{+cr}^* relies on the net Burgers vectors of shear dislocations $b_{x_1}^T$, on the net Burgers vectors of climbing dislocations $b_{x_2}^T$, and on the net Burgers vectors of electric dislocations b_φ^T inside the microcrack as shown in (4-3); while G_{-cr}^* relies on the net Burgers vectors of shear dislocations $d_{x_3}^T$ and on the net Burgers vectors of electric dislocations d_φ^T inside the microcrack as shown in Equation (4-1). We would like to assume that $b_{x_1}^T$, $b_{x_2}^T$, b_φ^T , $d_{x_3}^T$ and d_φ^T are material-dependent constants, which measure the magnitudes of the ductility and dielectricity of the matrix material. Also, it is very likely that after a microcrack is initiated, no more dislocations enter the crack, because the concentrated stress ahead of the rigid line tip has been released. Nonetheless, all these assumptions and conjectures need experimental support before pursuing further theoretical investigations.

In-plane case. If the rigid line isn't loaded with the tip shear stress field K_{II}^* , Equation (4-3) is reduced to

$$G_{+cr}^* = C_1 G_{+cr},$$

with

$$C_1 = -\frac{1}{2\pi^2} \frac{\mathbf{H}'_{11}}{\mathbf{s}^T \tilde{\mathbf{X}} \mathbf{s}}. \tag{4-5}$$

Equation (4-5) partially confirmed our initial conjecture in the first equation in (1-2), though only for very brittle materials under tensile stress and electric displacement fields. The numerical values of the coefficient C_1 for PZT-5H, PZT-4, PZT-5 and PZT-7A ceramics under the ratio $c/a = 10^{-4}$ are as follows:

PZT-5H	PZT-5	PZT-4	PZT-7A
5.931	17.651	12.158	10.355

The numerical values of the coefficient C_1 for PZT-5H for the ratio c/a are listed in Table 3. It is observed that, when the micro crack is at the very initial stage ($c/a < 10^{-3}$), the coefficient C_1 is constant. When the micro crack propagates further, the absolute value of the coefficient C_1 increases so slightly that we can still consider it a constant in the same solid. The C_1 value also indicates that the microcrack initiation is catastrophic.

For isotropic elastic materials, one finds

$$G_{+cr|iso}^* = C_{1|iso} G_{+cr|iso},$$

in which

$$C_{1|iso} = -\frac{3 - 4\nu}{(\sqrt{2\pi} F_1(1))^2 (1 - 2\nu)^2}.$$

It is worth mentioning that for the incompressible solid, $\nu = 0.5$, the numerical value of $C_{1|iso}$ approaches infinity, which indicates that the crack initiation is catastrophic.

It is noted that microcrack initiation at other angles may occur at the rigid line tip under some mixed loadings for the anti-plane and in-plane cases. The current approach can also be employed to analyze such cases, if the rigid line extension force is calculated as the mechanical strain energy released per infinitesimal translation in the inclined direction. However, the constants C_1 and C_2 may be different and need to be further investigated for different angles.

Appendix A

In a Cartesian coordinate system (x_1, x_2, x_3) , for a linear piezoelectric medium without body forces and with free charges at constant temperature, the constitutive and equilibrium equations given in [Tieresten 1969] are

$$\sigma_{ij} = c_{ijkl} u_{k,l} + e_{kji} \phi_{,k}, \quad D_i = e_{ikl} u_{k,l} - \varepsilon_{ik} \phi_{,k}, \quad i, j, k, l = 1, 2, 3, \tag{A-1}$$

$$\sigma_{ij,j} = 0, \quad D_{i,i} = 0, \quad i, j = 1, 2, 3, \tag{A-2}$$

where σ_{ij} , D_i , u_i , ϕ are the mechanical stress, electric displacement, elastic displacement and electric potential, while c_{ijkl} , e_{kij} , ε_{ij} are the elastic, piezoelectric and dielectric constants.

For a two-dimensional problem in which the variables depend on x_1 , x_2 only, a general solution to Equation (A-2), given in [Barnett and Lothe 1975], is

$$\mathbf{u} = \mathbf{a}f(z), \quad z = x_1 + px_2. \quad (\text{A-3})$$

Here f is an arbitrary function of z , while p and \mathbf{a} are determined by inserting (A-3) into (A-2). We have

$$[\mathbf{Q} + p(\mathbf{R} + \mathbf{R}^T) + p^2\mathbf{T}] \mathbf{a} = \mathbf{0}, \quad (\text{A-4})$$

where the matrices \mathbf{Q} , \mathbf{R} and \mathbf{T} are

$$\mathbf{Q} = \begin{bmatrix} c_{i1k1} & e_{i11} \\ e_{1k1}^T & -\varepsilon_{11} \end{bmatrix}, \quad \mathbf{R} = \begin{bmatrix} c_{i1k2} & e_{2i1} \\ e_{1k2}^T & -\varepsilon_{12} \end{bmatrix}, \quad \mathbf{T} = \begin{bmatrix} c_{i2k2} & e_{2i2} \\ e_{2k2}^T & -\varepsilon_{22} \end{bmatrix}.$$

The generalized stresses obtained by substituting (A-3) into (A-1) can be written in terms of the stress function Φ as

$$\{\sigma_{1j} \ D_1\}^T = -\Phi_{,2}, \quad \{\sigma_{2j} \ D_2\}^T = -\Phi_{,1},$$

in which

$$\Phi = \mathbf{b}f(z), \quad \mathbf{b} = (\mathbf{R}^T + p\mathbf{R}) \mathbf{a} = -p^{-1}(\mathbf{Q} + p\mathbf{R}) \mathbf{a}.$$

From (A-4) we see that eight eigenvalues p consist of four pairs of complex conjugates. If p_α , \mathbf{a}_α are the eigenvalues and the associated eigenvectors, we let

$$\begin{aligned} \text{Im}(p_\alpha) > 0, \quad p_{\alpha+4} = \bar{p}_\alpha, \\ \mathbf{a}_{\alpha+4} = \bar{\mathbf{a}}_\alpha, \quad \mathbf{b}_{\alpha+4} = \bar{\mathbf{b}}_\alpha, \quad \alpha = 1, 2, 3, 4, \end{aligned}$$

where Im stands for the imaginary part and the overbar denotes complex conjugation.

Assuming that p_α are distinct, the general solutions are obtained by

$$\mathbf{u} = 2 \text{Re} \left(\sum_{\alpha=1}^4 \mathbf{a}_\alpha f_\alpha(z_\alpha) \right), \quad \Phi = 2 \text{Re} \left(\sum_{\alpha=1}^4 \mathbf{b}_\alpha f_\alpha(z_\alpha) \right),$$

where Re stands for the real part, and

$$f_{\alpha+4} = \bar{f}_\alpha.$$

The 4×4 complex matrices \mathbf{A} and \mathbf{B} defined by

$$\mathbf{A} = [\mathbf{a}_1 \ \mathbf{a}_2 \ \mathbf{a}_3 \ \mathbf{a}_4], \quad \mathbf{B} = [\mathbf{b}_1 \ \mathbf{b}_2 \ \mathbf{b}_3 \ \mathbf{b}_4],$$

satisfy, when properly normalized, the orthogonality relation

$$\begin{bmatrix} \mathbf{B}^T & \mathbf{A}^T \\ \bar{\mathbf{B}}^T & \bar{\mathbf{A}}^T \end{bmatrix} \begin{bmatrix} \mathbf{A} & \bar{\mathbf{A}} \\ \mathbf{B} & \bar{\mathbf{B}} \end{bmatrix} = \begin{bmatrix} \mathbf{I} & \mathbf{O} \\ \mathbf{O} & \mathbf{I} \end{bmatrix}.$$

The matrices \mathbf{H} , \mathbf{L} and \mathbf{S} defined by

$$\begin{aligned} \mathbf{H} &= i2 \mathbf{A} \mathbf{A}^T, \\ \mathbf{L} &= i2 \mathbf{B} \mathbf{B}^T, \\ \mathbf{S} &= i (\mathbf{A} \mathbf{B}^T - \mathbf{I}) \end{aligned}$$

can be shown to be real. The matrices \mathbf{H} and \mathbf{L} are symmetric.

Appendix B

$$h_1(y, \zeta, a) = \sqrt{\frac{1}{y^2+4a^2}} \sqrt{\frac{\zeta y+4a^2}{2} + \frac{1}{2} P(y, \zeta, a)}$$

$$h_2(y, \zeta, a) = -\sqrt{\frac{1}{y^2+4a^2}} \sqrt{\frac{\zeta y-4a^2}{2} + \frac{1}{2} P(y, \zeta, a)}$$

$$h_3(y, \zeta, a) = \sqrt{\frac{\zeta}{y+\zeta}} \sqrt{\frac{1}{(y+\zeta)^2+4a^2}} \cdot \sqrt{\frac{\zeta(y+\zeta)+4a^2}{2} + \frac{1}{2} Q(y, \zeta, a)}$$

$$h_4(y, \zeta, a) = -\sqrt{\frac{\zeta}{y+\zeta}} \sqrt{\frac{1}{(y+\zeta)^2+4a^2}} \cdot \sqrt{\frac{\zeta(y+\zeta)-4a^2}{2} + \frac{1}{2} Q(y, \zeta, a)}$$

$$P(y, \zeta, a) = \sqrt{16a^4 + \zeta^2 y^2 + 4a^2(y^2 + \zeta^2)}$$

$$Q(y, \zeta, a) = \sqrt{16a^4 + \zeta^2(y + \zeta)^2 + 4a^2(y^2 + 2\zeta^2 + 2y\zeta)}$$

$$\begin{aligned} h_5(y, \zeta, a) &= -\frac{1}{y}(1 - h_3(y, \zeta, a)) - \frac{1}{y+\zeta} \left(1 - \sqrt{\frac{\zeta}{y}} h_2(y, \zeta, a) \right) \\ &\quad - \frac{1}{y+2\zeta} (1 + h_4(y, \zeta, a)) \end{aligned}$$

$$\tilde{h}_1(u, r, c/a) = \sqrt{\frac{r+1}{u+1}} h_1(u+1, r+1, a/c)$$

$$\tilde{h}_5(u, r, c/a) = \frac{1}{c} h_5(u+1, r+1, a/c).$$

Appendix C

$$\begin{aligned}
 \mathbf{X}_{11} &= \mathbf{L}'_{11}(f_{11})^2 \\
 \mathbf{X}_{22} &= \mathbf{L}'_{22}(f_{21})^2 + \mathbf{L}'_{23} f_{21} f_{31} \\
 \mathbf{X}_{23} &= \mathbf{X}_{32} = \mathbf{L}'_{22} f_{21} f_{22} + \frac{1}{2} \mathbf{L}'_{23}(f_{22} f_{31} + f_{21} f_{32}) \\
 \mathbf{X}_{33} &= \mathbf{L}'_{22}(f_{22})^2 + \mathbf{L}'_{23} f_{22} f_{32} \\
 \mathbf{Y}_{11} &= \mathbf{L}'_{11} f_{11} f_{12} \\
 \mathbf{Y}_{22} &= \mathbf{L}'_{22} f_{21} f_{23} + \frac{1}{2} \mathbf{L}'_{23}(f_{21} f_{33} + f_{31} f_{23}) \\
 \mathbf{Y}_{23} &= \mathbf{L}'_{22} f_{21} f_{24} + \frac{1}{2} \mathbf{L}'_{23}(f_{21} f_{34} + f_{31} f_{24}) \\
 \mathbf{Y}_{32} &= \mathbf{L}'_{22} f_{22} f_{23} + \frac{1}{2} \mathbf{L}'_{23}(f_{22} f_{33} + f_{32} f_{23}) \\
 \mathbf{Y}_{33} &= \mathbf{L}'_{22} f_{22} f_{24} + \frac{1}{2} \mathbf{L}'_{23}(f_{22} f_{34} + f_{32} f_{24}) \\
 \mathbf{Z}_{11} &= \mathbf{L}'_{11}(f_{12})^2 \\
 \mathbf{Z}_{22} &= \mathbf{L}'_{22}(f_{23})^2 + \mathbf{L}'_{23} f_{23} f_{33} \\
 \mathbf{Z}_{23} &= \mathbf{Z}_{32} = \mathbf{L}'_{22} f_{23} f_{24} + \frac{1}{2} \mathbf{L}'_{23}(f_{23} f_{34} + f_{24} f_{33}) \\
 \mathbf{Z}_{33} &= \mathbf{L}'_{22}(f_{24})^2 + (\tilde{\mathbf{L}}^{-1})_{33}(f_{34})^2 + \mathbf{L}'_{23} f_{24} f_{34}.
 \end{aligned}$$

References

- [Asundi and Deng 1995] A. Asundi and W. Deng, "Rigid inclusions on the interface between two bonded anisotropic media", *J. Mech. Phys. Solids* **43**:7 (1995), 1045–1058.
- [Ballarini 1990] R. Ballarini, "A rigid line inclusion at a bimaterial interface", *Eng. Fract. Mech.* **37**:1 (1990), 1–5.
- [Barnett and Lothe 1975] D. M. Barnett and J. Lothe, "Dislocations and line charges in anisotropic piezoelectric insulators", *Phys. Status Solidi B* **67**:1 (1975), 105–111.
- [Chen et al. 2005a] B. J. Chen, D. W. Shu, and Z. M. Xiao, "Dislocation interacting with collinear rigid lines in piezoelectric media", 2005. Submitted to *JomMS*.
- [Chen et al. 2005b] B. J. Chen, D. W. Shu, and Z. M. Xiao, "Electro-elastic interaction between a piezoelectric screw dislocation and collinear rigid lines", *Int. J. Eng. Sci.* **44**:7 (2005), 422–435.
- [Comninou 1977] M. Comninou, "The interface crack", *J. Appl. Mech. (ASME)* **44**:4 (1977), 631–636.
- [Deeg 1980] W. F. Deeg, *The analysis of dislocation, crack, and inclusion problems in piezoelectric solids*, Ph.D. thesis, Stanford University, 1980.
- [Deng and Meguid 1998] W. Deng and S. A. Meguid, "Analysis of conducting rigid inclusion at the interface of two dissimilar piezoelectric materials", *J. Appl. Mech. (ASME)* **65**:1 (1998), 76–84.
- [Dunn and Taya 1994] M. L. Dunn and M. Taya, "Electroelastic field concentrations in and around inhomogeneities in piezoelectric solids", *J. Appl. Mech. (ASME)* **61**:2 (1994), 474–475.
- [Erdogan et al. 1973] F. Erdogan, G. D. Gupta, and T. S. Cook, "Numerical solution of singular integral equations", pp. 368–425 in *Methods of Analysis and Solutions of Crack Problems*, edited by G. C. Sih, Noordhoff, Leyden, 1973.
- [Fan 1994] H. Fan, "Interfacial Zener-Stroh crack", *J. Appl. Mech. (ASME)* **61**:4 (1994), 829–834.
- [Fan and Keer 1993] H. Fan and L. M. Keer, "Two-dimensional line defects in anisotropic elastic solids", *Int. J. Fract.* **62**:1 (1993), 25–42.

- [Gao and Fan 2001] C. F. Gao and W. X. Fan, "An interface inclusion between two dissimilar piezoelectric materials", *Appl. Math. Mech.* **22**:1 (2001), 96–104. English edition.
- [He et al. 1991] M. Y. He, A. Bartlett, and A. G. Evans, "Kinking of a crack out of an interface: Role of in-plane stress", *J. Am. Ceram. Soc.* **74**:4 (1991), 767–771.
- [Kikuchi et al. 1981] M. Kikuchi, K. Shiozawa, and J. Weertman, "Void nucleation in astroloy: Theory and experiments", *Acta Metall.* **29**:10 (1981), 1747–1758.
- [Li and Ting 1989] Q. Li and T. C. T. Ting, "Line inclusions in anisotropic elastic solids", *J. Appl. Mech. (ASME)* **56**:3 (1989), 556–563.
- [Muskhelishvili 1977] N. I. Muskhelishvili, *Some basic problems of the mathematical theory of elasticity*, Noordhoff, Leyden, 1977.
- [Pak 1990] Y. E. Pak, "Crack extension force in a piezoelectric material", *J. Appl. Mech. (ASME)* **57**:3 (1990), 647–653.
- [Pak 1992] Y. E. Pak, "Linear electro-elastic fracture mechanics of piezoelectric materials", *Int. J. Fract.* **54**:1 (1992), 79–100.
- [Park and Sun 1993] S. B. Park and C. T. Sun, "Effect of electric field on fracture of piezoelectric ceramics", *Int. J. Fract.* **70**:3 (1993), 203–216.
- [Park and Sun 1995] S. B. Park and C. T. Sun, "Fracture criteria for piezoelectric ceramics", *J. Am. Ceram. Soc.* **78**:6 (1995), 1475–1480.
- [Shi 1997] W. C. Shi, "Rigid line inclusions under anti-plane deformation and in-plane electric field in piezoelectric materials", *Eng. Fract. Mech.* **56**:2 (1997), 265–274.
- [Suo et al. 1992] Z. Suo, C. M. Kuo, D. M. Barnett, and J. R. Willis, "Fracture mechanics for piezoelectric ceramics", *J. Mech. Phys. Solids* **40**:4 (1992), 739–765.
- [Tiersten 1969] H. F. Tiersten, *Linear piezoelectric plate vibration*, Plenum, New York, 1969.
- [Wang et al. 1985] Z. Y. Wang, H. T. Zhang, and Y. T. Chou, "Characteristics of the elastic field of a rigid line inhomogeneity", *J. Appl. Mech. (ASME)* **52**:4 (1985), 818–822.
- [Wang et al. 1986] Z. Y. Wang, H. T. Zhang, and Y. T. Chou, "Stress singularity at the tip of a rigid line inhomogeneity under antiplane shear loading", *J. Appl. Mech. (ASME)* **53**:2 (1986), 459–461.
- [Weertman 1986] J. Weertman, "Zener-Stroh crack, Zener-Hollomon parameter, and other topics", *J. Appl. Phys.* **60**:6 (1986), 1877–1887.
- [Xiao and Fan 1990] Z. M. Xiao and H. Fan, "Microcrack initiation at tip of a rigid line inhomogeneity", *Int. J. Fract.* **82**:1 (1990), 1–9.
- [Xiao et al. 2003] Z. M. Xiao, Y. Dai, and B. J. Chen, "Micro-crack initiation at tip of a rigid line inhomogeneity in piezoelectric materials", *Int. J. Eng. Sci.* **41**:2 (2003), 137–147.

Received 8 Dec 2005.

ZHONGMIN XIAO: mzxiao@ntu.edu.sg
 School of Mechanical & Aerospace Engineering, Nanyang Technological University,
 Nanyang Avenue, Singapore 639798

HONGXIA ZHANG: zh0001ia@ntu.edu.sg
 School of Mechanical & Aerospace Engineering, Nanyang Technological University,
 Nanyang Avenue, Singapore 639798

BINGJIN CHEN: mbjchen@ntu.edu.sg
 School of Mechanical & Aerospace Engineering, Nanyang Technological University,
 Nanyang Avenue, Singapore 639798

